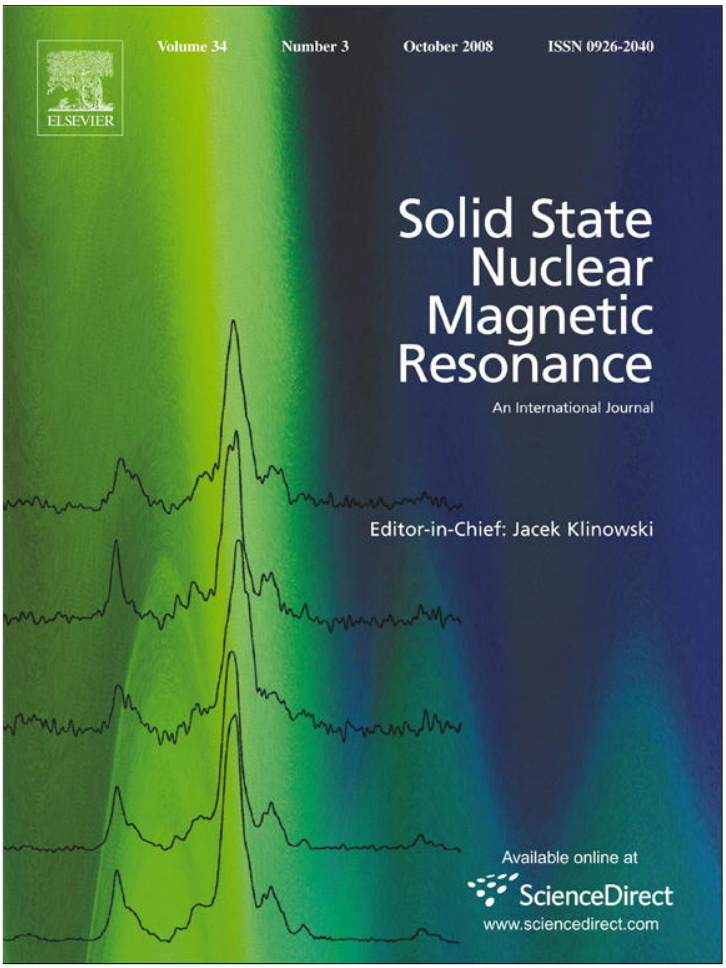

Solid State Nuclear Magnetic Resonance 34 (2008) 191–195

Contents lists available at ScienceDirect

Solid State Nuclear Magnetic Resonance

journal homepage: www.elsevier.com/locate/ssnmr

Derivation and evaluation of the fourth moment of NMR lineshape in zero-field

Vassilis Cutsuridis [a,*], Pawan K. Kahol [b]

[a] Department of Computing Science and Mathematics, University of Stirling, Stirling FK9 4LA, Scotland, UK
[b] Department of Physics, Astronomy, and Materials Science, Missouri State University, 901 S. National Avenue, Springfield, MO 65897, USA

ARTICLE INFO

Article history:
Received 17 April 2008
Received in revised form
20 August 2008
Available online 13 September 2008

PACS:
32.10.Dk
76.60.−k
82.56.−b
82.56.Dj
32.70.Jz
32.30.Dx

Keywords:
Nuclear magnetic resonance (NMR)
Zero-field NMR
Theory of moments
Fourth moment
Second moment

ABSTRACT

An expression for the fourth moment in zero-field NMR has been analytically derived and numerically evaluated for a rigid cubic lattice. Model simulations have been performed to calculate the second moment, the fourth moment, the ratio of the fourth moment to the square of the second moment, and the width of the resonance line for a crystal and a polycrystalline material in high-field as well as in zero-field NMR. The simulation results allow us to draw two conclusions: (1) zero-field NMR gives sharper and better defined spectra than the high-field NMR and (2) the ratio of the high- to zero-field resonance line-widths is 4 for a crystal, whereas it is 11 for a polycrystalline material.

1. Introduction

Nuclear magnetic resonance (NMR) is a very sophisticated technique, which helps with the study of the structure, internal motions, and phase transitions in solids, provided that nuclei in the studied material have spin $I>0$ [1]. Like all other spectroscopic methods [2], NMR allows the observation of a set of energy levels (here nuclear levels) by spectral absorption or emission of rf photons. NMR experiments were successfully performed independently by two research groups [3,4] in 1945. Many new methods of NMR spectroscopy have since been developed to improve sensitivity and the resolution of the NMR spectra. One such method is the zero-field NMR (ZF-NMR) [5,6].

In the ZF-NMR, the nuclear spins of the sample are first strongly polarized in the high magnetic field of a spectrometer. The sample is then moved slowly into a much smaller magnetic field. The field is reduced to zero for a period t_1 which is around 1 μs. In the absence of the magnetic field, the polarized nuclei undergo a process called zero-field free precession. After a time t_1, the field is switched back on and the sample is moved back into the high-field for detection of the signal. The entire procedure is repeated for regularly incremented values of t_1. The advantage of ZF-NMR is that there is no orientation dependence of the energy levels in zero magnetic field. That is, each crystallite has the same energy level structure and therefore, can give rise to only one set of transition frequencies. Therefore, the spectra are sharp and well-defined provided that there are only two or three spins in the system.

However, if the number of interacting spins is increased, the resulting spectrum, even in zero-field, is broad and featureless like the one observed in high-fields. The question that we address in this paper is the following: How broad is the NMR line-width in zero-field compared to its value in high-field? To our knowledge this problem has not been discussed earlier. For specific lineshapes, such as Gaussian or truncated-Lorentzian, the full-width at half-height (FWHH) is exactly defined in terms of second and fourth moments. In fact, there also exists an expression which connects a universal lineshape with the lower order moments [7]. For a given Hamiltonian, moments are related to a material's structure and can be exactly calculated. For the dipolar

* Corresponding author. Fax: +44 1786 464551.
E-mail address: vcu@cs.stir.ac.uk (V. Cutsuridis).

0926-2040/$ - see front matter © 2008 Elsevier Inc. All rights reserved.
doi:10.1016/j.ssnmr.2008.08.004

interactions considered in our paper, orientation dependence of the interactions contributes to the high-field line but not to the zero-field line. Once an "unstructured" line is obtained, whether in high-field or in zero-field, one must resort to the methodology of moments to deduce structural information from the observed lineshape.

The objective of this paper is thus to quantify FWHH in the high- and zero-field situations which we have done using the concept of moments. To accomplish this objective, we have derived an expression of the fourth moment in ZF-NMR (Appendix), numerically evaluated second and fourth moments, their ratio and the line-widths in both high- and zero-fields. We compare the calculated results in Section 3 and draw conclusions regarding the zero-field NMR method in Section 4.

2. Theoretical background

The method of moments is a clever technique developed by Van Vleck [8], which enables one to compute properties of the resonance line without solving explicitly for the eigenstates and the eigenvalues of the energy. The shape of a resonance line is given by

$$f(\omega) = \sum_{a,b} |(a|\mu_x|b)|^2 \cdot \delta(E_a - E_b - \hbar\omega) \tag{1}$$

where μ_x is the magnetic moment in the x-direction, E_a and E_b are the energies of the $|a\rangle$ and $|b\rangle$ states, and δ is the delta function. The moments of the resonance line $f(\omega)$ are then defined by the equation

$$\langle\omega^n\rangle = \frac{\int_0^\infty \omega^n f(\omega)\mathrm{d}\omega}{\int_0^\infty f(\omega)\mathrm{d}\omega} \tag{2}$$

In particular the lower order moments up to the fourth are defined as

$$\begin{aligned}
\langle\omega^0\rangle &= 1\\
\langle\omega^2\rangle &= \frac{\int_0^\infty \omega^2 f(\omega)\mathrm{d}\omega}{\int_0^\infty f(\omega)\mathrm{d}\omega} = -\frac{Tr[H,I_x]^2}{Tr[I_x^2]}\\
\langle\omega^4\rangle &= \frac{\int_0^\infty \omega^4 f(\omega)\mathrm{d}\omega}{\int_0^\infty f(\omega)\mathrm{d}\omega} = \frac{Tr[H,[H,I_x]]^2}{Tr[I_x^2]}
\end{aligned} \tag{3}$$

The odd-order moments vanish since the resonance line is symmetrical. The line-width of the NMR spectrum is then given by

$$\delta = \sqrt{\pi \frac{M_2}{2((M_4/M_2^2) - 1)}} \tag{4}$$

where M_2 and M_4 are the second and fourth moments, respectively. That is, the lower order moments define the line-width [7].

As we mentioned earlier for ZF-NMR, the polarized nuclei undergo a process called zero-field free precession in zero-field, which is repeated for regularly incremented values of time, t_1. The resulting free induction decay signal is usually written in terms of the lower order moments [9] as

$$G(t) = 1 - M_2\frac{t^2}{2!} + M_4\frac{t^4}{4!} + \ldots \tag{5}$$

The zeroth and second moment in zero-field are then given by

$$\begin{aligned}
\langle\omega^0\rangle &= 1\\
\langle\omega^2\rangle &= \frac{\int_0^\infty \omega^2 f(\omega)\mathrm{d}\omega}{\int_0^\infty f(\omega)\mathrm{d}\omega} = -\frac{Tr[H,I_x]^2}{Tr[I_x^2]}\\
&= \frac{3}{4}\gamma^4\hbar^2 I(I+1)\sum_k \frac{(1-3\cos^2\theta_{jk})^2}{r_{jk}^6}
\end{aligned} \tag{6}$$

However, an expression for the fourth moment in zero-field NMR has not been derived yet, and hence the numerical evaluation of the ZF-NMR line-width is impossible. An expression of the fourth moment in ZF-NMR is derived in the appendix. Numerical evaluations of the second, the fourth moment and the line-width in high-field and zero-field NMR for a single crystal and a polycrystalline material are detailed in the next section.

3. Numerical analysis

The numerical evaluations of the second and fourth moments in zero- and high-field NMR are presented in this section. The evaluations were performed on a model rigid lattice, the spatial structure of which is depicted in Fig. 1. The central atom of this crystal is considered to be the point of origin and equal number of atoms is placed in all directions. A magnetic field, H, is placed in the z-direction. The internuclear distance, r, is defined as the distance from the point of origin to every other atom in the lattice. The polar angle θ is measured as the angle the internuclear distance makes with the applied magnetic field and the azimuth angle φ is the angle the interneuclear distance makes with the x–y plane. The internuclear distance and the polar and azimuth angles are calculated for every atom in the lattice since they are necessary for the evaluation of the second and fourth moments in both the high- and zero-field cases.

3.1. Crystal second and fourth moments in high-field NMR

The second and fourth moments in the high-field NMR [10] are given by

$$M_2 = \frac{3}{4}I(I+1)\gamma^4\hbar^2\sum_k \frac{(1-3\cos^2\theta_{0k})^2}{r_{0k}^6} \tag{7}$$

$$M_4 = \gamma^8\hbar^4\left\{\left\{3\left(\sum_k b_{0k}^2\right)^2 - \frac{1}{3}\sum_{kl\neq} b_{0k}^2(b_{0l}^2 - b_{kl}^2)^2 - 2\sum_k b_{0k}^4\right\} \times \left[\frac{I(I+1)}{3}\right]^2\right. \tag{8}$$

where

$$b = \frac{(1-3\cos^2\theta)}{r^3}$$

Both moments as well as the ratio of the fourth moment to the square of the second moment and the width of the resonance line (Eq. (4)) were numerically evaluated for three different directions of the magnetic field: (1) along the z-direction (1 0 0), (2) along the x–y plane (1 1 0) and (3) along the crystal diagonal (1 1 1). The

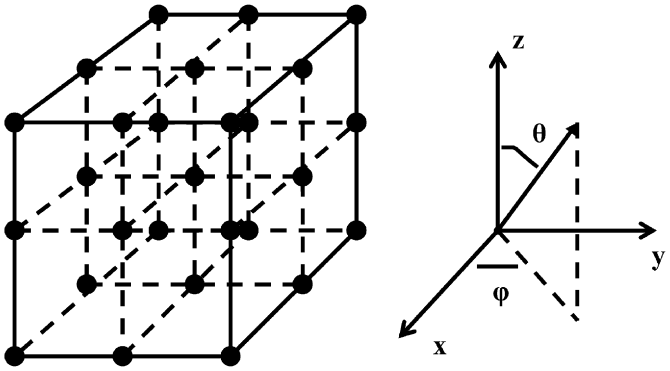

Fig. 1. Model cubic lattice structure with equal number of atoms placed in all possible directions.

Table 1
High-field and zero-field values of the second moment, the fourth moment, their ratio and the linewidth of a crystal lattice

Crvsial (−5:1:5)	High magnetic field (100)	High magnetic field (110)	High magnetic field (111)	Zero magnetic field (−2:1:2)	Zero magnetic field (−4:1:4)	Zero magnetic field (−6:1:6)	Zero magnetic field (−8:1:8)
$M_2(\gamma^4\hbar^2)$	7.51	2.84	1.29	7.43	7.5	7.51	7.51
$M_4(\gamma^8\hbar^4)$	119.61	18.58	3.92	684.82	813.24	865.43	895.79
$M_4M_2)^2$	2.12(2.07)	2.3(2.22)	2.37(2.3)	12.4	14.46	15.35	15.88
Linewidth ($\gamma^2\hbar$)	3.24	1.85	1.22	1.01	0.94	0.91	0.89

In the high-field case, the magnetic field was oriented in three spatial directions: (l) along the z-axis (110). (2) Along the x–y plane (110) and (3) along the crystal diagonal (111). Values in parenthesis are the experimental ones from [10, pp. 112–113].

value of the spin used was $\frac{1}{2}$. The number of atoms placed along the positive and negative x-, y- and z-directions in our cubic lattice was six. For each atom in the lattice structure the distance r and the polar angle θ from the central atom were estimated. The simulation results are summarized in Table 1. The ratio of the fourth moment to the square of the second moment was found to be 2.12 for the 100 direction, 2.3 for the 110 direction and 2.37 for the 111 direction. The approximate values evaluated by Van Vleck were 2.07, 2.22 and 2.3 in the respected magnetic field direction ([10, p.113]). The width values for the resonance lines were found to be $3.24\gamma^2\hbar$ for the 100 direction, $1.85\gamma^2\hbar$ for the 110 direction and $1.22\gamma^2\hbar$ for the 111 direction.

3.2. Polycrystalline second and fourth moment in high-field NMR

To numerically evaluate the second and fourth moment for a polycrystalline material all possible directions in space for a crystallite had to be considered. Instead of rotating our crystal and holding the magnetic field along the z-direction, we held the crystal fixed and rotated the magnetic field [11,12]. Two angles α and β, one with respect to the z-axis and the other one with respect to the x–y plane were used to cover all possible directions of the magnetic field in space (Fig. 2). The angles α and β were allowed to vary from 0 to 2π and from 0 to π, respectively. The angle value range was then divided into n sub-intervals equal to the number of rotations. The number of atoms in the crystal structure was once again set to 6.

The expression of the spatial averaged second moment of a rigid lattice without internal motions used was derived using Goc's methodology [12]

$$M_2 = \frac{3}{4} I(I+1)\left\langle B^2 \right\rangle$$

where

$$\left\langle B^2 \right\rangle = \frac{\sum_{k=0}^{N-1} W \mathrm{d}\alpha}{2 \cdot N}$$

and

$$\begin{aligned} W = {} & c_1 \cos^4\alpha + c_2 \sin^4\alpha + c_3 + c_4 \sin^2\alpha\cos^2\alpha + c_5 \cos^2\alpha \\ & + c_6 \sin^2\alpha + c_{12} \sin^2\delta\cos^2\delta + c_{12}\cos^2\delta + c_{14} \sin\delta\cos^3\delta \\ & + c_{17}\cos^2\delta + c_{23}\sin^2\delta + c_{24}\sin^3\delta\cos\delta + c_{27}\sin^2\delta \\ & + c_{34} \sin\delta\cos\delta + c_{37} + c_{47} \sin\delta\cos\delta + c_{56}\sin\delta\cos\delta \end{aligned}$$

with

$$\begin{aligned} & c_1 = \tfrac{16}{15}a_1^2, \quad c_2 = \tfrac{16}{5}a_2^2, \quad c_3 = \tfrac{2}{5}a_3^2, \quad c_4 = \tfrac{16}{15}a_4^2 \\ & c_5 = \tfrac{4}{15}a_5^2, \quad c_6 = \tfrac{4}{15}a_6^2, \quad c_7 = 2a_7^2, \quad c_{12} = \tfrac{32}{15}a_1a_2 \\ & c_{13} = \tfrac{8}{15}a_1a_3, \quad c_{14} = \tfrac{32}{15}a_1a_4, \quad c_{17} = -\tfrac{8}{3}a_1a_7, \\ & c_{23} = \tfrac{8}{15}a_2a_3, \quad c_{24} = \tfrac{32}{15}a_2a_4, \quad c_{27} = -\tfrac{8}{3}a_2a_7, \quad c_{34} = \tfrac{8}{15}a_3a_4, \\ & c_{37} = -\tfrac{4}{3}a_3a_7, \quad c_{47} = -\tfrac{8}{3}a_4a_7, \quad c_{56} = \tfrac{8}{15}a_5a_6 \end{aligned}$$

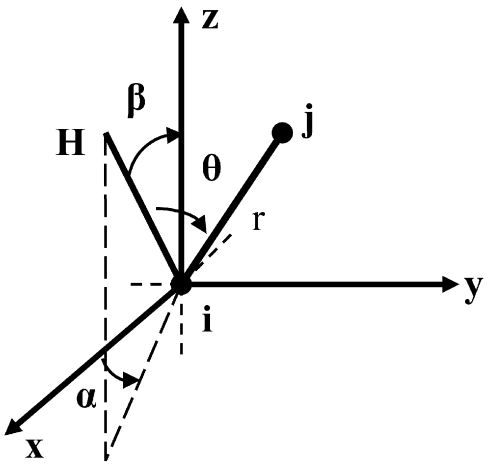

Fig. 2. Schematic representation of spatial arrangement of atoms in the model lattice. The position of the atom i is denoted in the Cartesian coordinate system as the point of origin, whereas the position of the atom j is denoted by x_j, y_j and z_j. The direction of the magnetic field H is defined by the polar angle β and the azimuth angle α in the same coordinate system.

and

$$\begin{aligned} & a_1 = 3(x_i - x_j)^2 r_{ij}^{-5}, \quad a_2 = 3(y_i - y_j)^2 r_{ij}^{-5}, \\ & a_3 = 3(z_i - z_j)^2 r_{ij}^{-5}, \quad a_4 = 6(x_i - x_j)(y_i - y_j) r_{ij}^{-5}, \\ & a_5 = 6(x_i - x_j)(z_i - z_j) r_{ij}^{-5}, \quad a_6 = 6(y_i - y_j)(z_i - z_j) r_{ij}^{-5}, \quad a_7 = r_{ij}^{-3} \end{aligned}$$

For 50 rotations of the magnetic field (see Table 2), the second moment for a polycrystalline material (powder) was calculated to be 3.8 $\gamma^4\hbar^2$, which is exactly equal to the predicted value by Van Vleck ([10, p. 112]). The fourth moment was calculated to be 48.33 $\gamma^8\hbar^4$. The ratio of the two moments and the width of the resonance line were thus obtained to be 3.34 and 1.58 $\gamma^2\hbar$, respectively.

3.3. Crystal second and fourth moments in ZF-NMR

In ZF-NMR the applied magnetic field is briefly removed for a short period of time. During that time the spins rotate freely in space. Since there is no angular dependence with the magnetic field, the polar angle θ is measured as the angle, the internuclear distance r makes with the z-axis. The two fourth moments (Eqs. (7) and (16), respectively), their ratio and the resonance line-width are evaluated for different number of atoms in the lattice. The simulation results are depicted in Table 1. It is clearly seen that as the number of atoms in the lattice is increased the moments, their ratio and the line-width converge to 7.51 $\gamma^4\hbar^2$, 895.79 $\gamma^8\hbar^4$, 15.88 and 0.89 $\gamma^2\hbar$, respectively. This is understandable since the most distant spins from the central spin

Table 2
High-field and zero-field values of the second moment, the fourth moment, their ratio and the linewidth of a powder

Powder	High magnetic field (−6:1:6) (50 rotations)	Zero magnetic field (−2:1:2) (50 rotations)	Zero magnetic field (−4:1:4) (50 rotations)	Zero magnetic field (−6:1:6) (50 rotations)
$M_2(\gamma^4\hbar^2)$	3.8 (3.8)	3.71	3.78	3.8
$M_4(\gamma^8\hbar^4)$	48.33	4.03×10^3	4.03×10^3	4.07×10^3
$M_4M_2)^2$	3.34	272.65	283.42	285.11
Linewidth ($\gamma^2\hbar$)	1.58	0.15	0.14	0.14

Values in parenthesis are the experimental ones from [10, pp. 112–113].

(origin) contribute less to the evaluated expression. The ratio of the high-field and zero-field line-widths was found to be 4:1.

3.4. Polycrystalline second and fourth moment in ZF-NMR

For a polycrystalline material in ZF-NMR all possible rotations in the space of the crystal had to be taken under consideration. The rotation matrix used to transform our coordinate system was

$$R=\begin{bmatrix} \cos\gamma\cos\beta\cos\alpha-\sin\gamma\sin\alpha & \cos\gamma\cos\beta\sin\alpha+\sin\gamma\cos\alpha & -\cos\gamma\sin\beta \\ -\sin\gamma\cos\beta\cos\alpha-\cos\gamma\sin\alpha & -\sin\gamma\cos\beta\sin\alpha+\cos\gamma\cos\alpha & \sin\gamma\sin\beta \\ \sin\beta\cos\alpha & \sin\beta\sin\alpha & \cos\beta \end{bmatrix} \tag{9}$$

The angles α, β and γ varied from 0 to 2π, from 0 to π and from 0 to 2π, respectively. The crystal was rotated 50 times and each time the second and fourth moments, their ratio and the line-width were evaluated for different number of atoms in the lattice. The simulation results are summarized in Table 2. As the number of atoms in the lattice grew, the values of the moments converged to 3.8 $\gamma^4\hbar^2$ and 4.07×10^3 $\gamma^8\hbar^4$. The value of the width of the resonance line of polycrystalline material converged to 0.14 $\gamma^2\hbar$. Finally, the ratio of the high-field and zero-field line-widths was estimated to be 11:1.

4. Conclusions

On the basis of the model ZF-NMR calculations presented in this paper, we are able to draw the following conclusions: (1) an analytic expression of the fourth moment in ZF-NMR has been derived, (2) numerical evaluations via computer simulations of the fourth moment, the ratio of the fourth moment to the square of the second moment and the resonance line-width in ZF-NMR for a crystal and a polycrystalline material were obtained, (3) we showed that the spectra using the ZF-NMR method are sharper when compared to the broad and largely unresolved spectra obtained from the high-field NMR method and (4) the ratio of the high- and zero-field resonance line-widths is 4:1 for a crystal, whereas for a polycrystalline material is 11:1.We therefore take the view that zero-field spectra are more amenable to obtaining better structural information of a material than the high-field spectra.

Acknowledgments

VC would like to thank the Informatics and Telecommunications Institute of the National Center for Scientific Research "Demokritos" in Greece for its computational facilities used during the numerical evaluation of this research. A part of this paper was submitted to Wichita State University as a Master's Thesis in 1996 [11].

Appendix A. Derivation of the fourth moment in ZF-NMR

We start the calculation of the fourth moment in ZF-NMR from the equation of the fourth moment in high-field NMR [10]

$$M_4=\frac{Tr[H,[H,I_z]]^2}{Tr[I_z^2]} \tag{10}$$

The Hamiltonian used in this relation is the full dipolar Hamiltonian [10]

$$H=\gamma^2\hbar\sum_{i<j}r_{ij}^{-3}O_{ij} \tag{11}$$

where

$$O_{ij}=a_1^{ij}A_1^{ij}+a_2^{ij}A_2^{ij}+a_3^{ij}A_3^{ij}+a_4^{ij}A_4^{ij}+a_5^{ij}A_5^{ij}$$

and

$$a_1^{ij}=\tfrac{1}{2}(1-3\cos^2\theta)$$
$$a_2^{ij}=-\tfrac{3}{2}\sin\theta\cos\theta\cdot e^{-i\phi}$$
$$a_3^{ij}=-\tfrac{3}{2}\sin\theta\cos\theta\cdot e^{i\phi}$$
$$a_4^{ij}=-\tfrac{3}{4}\sin^2\theta\cdot e^{-2i\phi}$$
$$a_5^{ij}=-\tfrac{3}{4}\sin^2\theta\cdot e^{2i\phi}$$

$$A_1^{ij}=3I_{zi}I_{zj}-I_iI_j$$
$$A_2^{ij}=I_{zi}I_{+j}+I_{zj}I_{+i}$$
$$A_3^{ij}=I_{zi}I_{-j}+I_{zj}I_{-i}$$
$$A_4^{ij}=I_{+i}I_{+j}$$
$$A_5^{ij}=I_{-i}I_{-j}$$

Substituting Eq. (11) back in Eq. (10), the numerator of the fourth moment becomes

$$[H,[H,I_z]]=\left[\sum_{i<j}O^{ij}\left[\sum_{k>l}O^{kl},\sum_m I_{zm}\right]\right]=\sum_{k>l}\left[O^{kl},\left[O^{kl},\sum_m I_{zm}\right]\right]+\sum_{k>l}^{i\neq k,l}\left[O^{ik}+O^{il},\left[O^{kl},\sum_m I_{zm}\right]\right] \tag{12}$$

Using the following commutation relations of quantum mechanics [13]

$$[I_x,I_y]=iI_z,\quad [I_+,I_z]=-I_+,\quad [I_-,I_x]=-I_z$$
$$[I_y,I_z]=iI_x,\quad [I_-,I_z]=I_-,\quad [I_+,I_y]=iI_z$$
$$[I_z,I_x]=iI_y,\quad [I_+,I_x]=I_z,\quad [I_-,I_y]=iI_z \tag{13}$$

and evaluating the first term of Eq. (12), we get

$$\left[O^{kl},\left[O^{kl},\sum_m I_{zm}\right]\right]=\left[\frac{1}{3}S(S+1)\right]^3\sum_{k\neq l}F_1+\left[\frac{1}{3}S(S+1)\right]^2\sum_{k\neq l}F_2+\left[\frac{1}{3}S(S+1)\right]^3\sum_{klj\neq}F_3 \tag{14}$$

where

$$F_1 = \frac{1152}{5}(f_1^{kl}f_4^{kl})^2 + \frac{864}{5}f_1^{kl}f_4^{kl}(f_2^{kl})^2 + \frac{504}{5}(f_1^{kl}f_2^{kl})^2 + \frac{3552}{5}(f_2^{kl}f_4^{kl})^2 + 96(f_2^{kl})^4 + \frac{3072}{5}(f_4^{kl})^4$$

$$F_2 = -\frac{144}{5}(f_1^{kl}f_4^{kl})^2 - \frac{104}{5}(f_2^{kl}f_4^{kl})^2 - \frac{64}{5}(f_4^{kl})^4 - \frac{18}{5}(f_1^{kl}f_2^{kl})^2 + \frac{72}{5}f_1^{kl}f_4^{kl}(f_2^{kl})^2 - 8(f_2^{kl})^4$$

$$F_3 = [36f_1^{kl}f_1^{jk}f_2^{kl}f_2^{jk} + 72f_1^{kl}f_2^{kl}f_2^{jk}f_4^{jk} + 72f_1^{jk}f_2^{kl}f_2^{jk}f_4^{kl} + 144f_2^{kl}f_2^{jk}f_4^{kl}f_4^{jk}]\cos(\phi_{kl} - \phi_{ik}) + 16[f_2^{kl}f_2^{jk}]^2 + 64[f_2^{kl}f_4^{jk}]^2 + 64[f_2^{jk}f_4^{kl}]^2 + 256[f_4^{kl}f_4^{jk}]^2$$

$$f_1 = \frac{1}{2}(1 - 3\cos^2\theta)\gamma^2\hbar^2 r^{-3}$$

$$f_2 = -\frac{3}{2}\sin\theta\cos\theta\gamma^2\hbar^2 r^{-3}$$

$$f_4 = -\frac{3}{4}\sin^2\theta\gamma^2\hbar^2 r^{-3}$$

Evaluating the second term of Eq. (12) and working out the mathematics gives us

$$\begin{aligned}
&\left[O^{ik} + O^{il}, O^{kl}, \sum_m I_{zm}\right] \\
&= \sum_{i\neq k\neq l}(-96f_1^{ik}f_1^{kl}f_2^{il}f_2^{kl}f_4^{kl} + 48f_1^{kl}f_2^{il}f_2^{kl}f_4^{il} + 128f_2^{kl}f_2^{il}f_4^{ik}f_4^{ik} + 20f_1^{kl}f_1^{il}f_2^{il}f_2^{kl} \\
&\quad + 8f_1^{ik}f_1^{ik}f_2^{il}f_2^{kl} + 8f_1^{ik}f_1^{il}f_2^{il}f_2^{kl} + 32f_2^{kl}f_2^{il}f_2^{ik}f_2^{ik})\cos(\phi_{kl} - \phi_{il}) \\
&\quad + (-48f_1^{kl}f_2^{il}f_2^{il}f_4^{kl} - 96f_1^{ik}f_2^{il}f_2^{il}f_4^{kl} + 144f_2^{ik}f_2^{ik}f_4^{kl}f_4^{il} - 16f_2^{ik}f_2^{kl}f_4^{ik}f_4^{il} \\
&\quad + 32f_1^{kl}f_1^{il}f_4^{il}f_4^{kl} + 128f_1^{ik}f_1^{ik}f_4^{il}f_4^{kl} + 128f_1^{ik}f_1^{il}f_4^{il}f_4^{kl})\cos 2(\phi_{kl} - \phi_{il}) \\
&\quad - 32f_2^{il}f_2^{ik}f_4^{il}f_4^{kl}\cos(3\phi_{il} - 2\phi_{kl} - \phi_{ik}) + 272(f_2^{ik}f_4^{kl})^2 + 256(f_4^{ik}f_4^{kl})^2 \\
&\quad + 32(f_2^{ik}f_2^{kl})^2 + 160(f_1^{ik}f_4^{kl})^2 + 28(f_1^{ik}f_2^{kl})^2 + 8f_1^{ik}f_1^{kl}f_2^{il}f_2^{il} + 128f_1^{ik}f_1^{il}f_2^{kl}f_2^{kl} \\
&\quad + (-96f_1^{ik}f_2^{kl}f_2^{il}f_4^{ik} - 256f_2^{il}f_2^{kl}f_4^{il}f_4^{ik} - 48f_1^{kl}f_1^{il}f_2^{il}f_4^{ik})\cos(\phi_{kl} + \phi_{il} - 2\phi_{ik}) \\
&\quad + 16\left\{\sum_{jkl\neq} f_2^{ik}f_2^{kl}\cos(\phi_{kl} - \phi_{ik})\right\}^2 + 16\left\{\sum_{jkl\neq} f_2^{ik}f_4^{kl}\cos(2\phi_{kl} + \phi_{ik})\right\}^2 \\
&\quad + 16\left\{\sum_{jkl\neq} f_2^{ik}f_4^{kl}\sin(2\phi_{kl} + \phi_{ik})\right\}^2 \qquad (15)
\end{aligned}$$

Combining the results from Eqs. (14) and (15) we get an expression for the fourth moment in ZF-NMR

$$\begin{aligned}
M_4 &= \frac{1}{N}\left[\frac{I(I+1)}{3}\right]^3\sum_{k\neq l}F_1 + \frac{1}{N}\left[\frac{I(I+1)}{3}\right]^2\sum_{k\neq l}F_2 \\
&\quad + \frac{1}{N}\left[\frac{I(I+1)}{3}\right]^3\{F_8\} + \frac{1}{N}\left[\frac{I(I+1)}{3}\right]^3\sum_{jkl\neq}\{F_3\cos(\phi_{kl} - \phi_{il}) \\
&\quad + F_4\cos 2(\phi_{kl} - \phi_{il}) + F_5\cos(\phi_{kl} + \phi_{il} - 2\phi_{ik}) \\
&\quad + F_6\cos(3\phi_{il} - 2\phi_{kl} - \phi_{ik}) + F_7\} \qquad (16)
\end{aligned}$$

where

$$F_1 = \frac{1152}{5}(f_1^{kl}f_4^{kl})^2 + \frac{864}{5}f_1^{kl}f_4^{kl}(f_2^{kl})^2 + \frac{504}{5}(f_1^{kl}f_2^{kl})^2 + \frac{3552}{5}(f_2^{kl}f_4^{kl})^2 + 96(f_2^{kl})^4 + \frac{3072}{5}(f_4^{kl})^4$$

$$F_2 = -\frac{144}{5}(f_1^{kl}f_4^{kl})^2 - \frac{104}{5}(f_2^{kl}f_4^{kl})^2 - \frac{64}{5}(f_4^{kl})^4 - \frac{18}{5}(f_1^{kl}f_2^{kl})^2 + \frac{72}{5}f_1^{kl}f_4^{kl}(f_2^{kl})^2 - 8(f_2^{kl})^4$$

$$\begin{aligned}
F_3 = &-96f_1^{ik}f_2^{kl}f_2^{il}f_4^{kl} + 120f_1^{kl}f_2^{il}f_2^{kl}f_4^{il} + 48f_1^{ik}f_2^{il}f_2^{kl}f_4^{il} \\
&+ 128f_2^{kl}f_2^{il}f_4^{ik}f_4^{ik} + 56f_1^{kl}f_1^{il}f_2^{il}f_2^{kl} + 8f_1^{ik}f_1^{il}f_2^{il}f_2^{kl} \\
&+ 8f_1^{ik}f1_1^{il}f_2^{il}f_2^{kl} + 32f_2^{kl}f_2^{ik}f_2^{il}f_2^{ik} + 72f_1^{il}f_2^{il}f_2^{kl}f_4^{kl} \\
&+ 144f_2^{kl}f_2^{il}f_4^{kl}f_4^{il}
\end{aligned}$$

$$\begin{aligned}
F_4 = &-48f_1^{kl}f_2^{il}f_2^{il}f_4^{kl} - 96f_1^{ik}f_2^{il}f_2^{il}f_4^{kl} + 144f_2^{ik}f_2^{ik}f_4^{kl}f_4^{il} \\
&- 16f_2^{ik}f_2^{kl}f_4^{ik}f_4^{il} + 32f_1^{kl}f_1^{il}f_4^{il}f_4^{kl} \\
&+ 128f_1^{ik}f_1^{ik}f_4^{il}f_4^{kl} + 128f_1^{ik}f_1^{il}f_4^{il}f_4^{kl}
\end{aligned}$$

$$F_5 = -96f_1^{ik}f_2^{kl}f_2^{il}f_4^{ik} - 256f_2^{il}f_2^{kl}f_4^{il}f_4^{ik} - 48f_1^{kl}f_2^{il}f_2^{kl}f_4^{ik}$$

$$F_6 = -32f_2^{il}f_2^{ik}f_4^{il}f_4^{kl}$$

$$\begin{aligned}
F_7 = &\,400(f_2^{ik}f_4^{kl})^2 + 512(f_4^{ik}f_4^{kl})^2 + 48(f_2^{ik}f_2^{kl})^2 \\
&+ 160(f_1^{ik}f_4^{kl})^2 + 28(f_1^{ik}f_2^{kl})^2 \\
&+ 8f_1^{ik}f_1^{kl}f_2^{il}f_2^{il} + 128f_1^{ik}f_1^{il}f_4^{kl}f_4^{kl}
\end{aligned}$$

$$F_8 = 16\left\{\sum_{jkl\neq} f_2^{ik}f_2^{kl}\cos(\phi_{kl} - \phi_{ik})\right\}^2 + 16\left\{\sum_{jkl\neq} f_2^{ik}f_4^{kl}\cos(2\phi_{kl} + \phi_{ik})\right\}^2 + 16\left\{\sum_{jkl\neq} f_2^{ik}f_4^{kl}\sin(2\phi_{kl} + \phi_{ik})\right\}^2$$

References

[1] R. Goc, Solid State Nucl. Magn. Res. 13 (1998) 55–61.
[2] U. Gonser, Microscopic Methods in Metals, Springer, Berlin, 1986.
[3] E.M. Purcell, H.C. Torrey, R.V. Pound, Phys. Rev. 69 (1946) 37.
[4] F. Bloch, W.W. Hansen, M. Packard, Phys. Rev. 69 (1946) 127.
[5] D.P. Weitekamp, A. Bielecki, D. Zax, K. Zilm, A. Pines, Phys. Rev. Lett. 50 (1983) 22.
[6] A.M. Thayer, A. Pines, Acc. Chem. Res. 20 (2) (1987) 47–53.
[7] M. Mehring, Principles of High Resolution NMR in Solids, second ed., Springer, New York Berlin Heidelberg, 1983.
[8] J.H. Van Vleck, Phys. Rev. 74 (9) (1948) 1168–1183.
[9] P.K. Kahol, Phys. Status Solidi (b) 159 (1990) 873.
[10] A. Abragam, Principles of Nuclear Magnetism, Oxford University Press, London, 1983.
[11] V. Cutsuridis, Calculation and study of the fourth moment in zero-field NMR. M.Sc. thesis, Wichita State University, 1996.
[12] R. Goc, J. Magn. Res. 132 (1998) 78–80.
[13] E.E. Anderson, Modern Physics and Quantum Mechanics, W.B. Saunders Company, 1970.